

1 **Method Note/**

2 **Influence of Pressure Change during Hydraulic Tests on Fracture**
3 **Aperture**

4
5
6
7
8
9 Sung-Hoon Ji^a*, Yong-Kwon Koh^a, Kristopher L. Kuhlman^b, Moo Yul Lee^c, and Jong
10 Won Choi^a

11
12
13
14 ^a *Radwaste Disposal Technology Development Division, Korea Atomic Energy*
15 *Research Institute, Daejeon, Republic of Korea*

16 ^b *Repository Performance Dept., Sandia National Laboratories, Carlsbad, NM, USA*

17 ^c *Geomechanics Dept., Sandia National Laboratories, Albuquerque, NM, USA*

18
19
20
21
22 * Corresponding author. Tel.: +82-42-868-4920; fax: +82-42-868-2064. *E-mail address:*
23 shji@kaeri.re.kr

32

33

34 **Abstract**

35 In a series of field experiments, we evaluate the influence of a small water pressure
36 change on fracture aperture during a hydraulic test. An experimental borehole is
37 instrumented at the Korea Atomic Energy Research Institute (KAERI) Underground
38 Research Tunnel (KURT). The target fracture for testing was found from the analyses
39 of borehole logging and hydraulic tests. A double packer system was developed and
40 installed in the test borehole to directly observe the aperture change due to water
41 pressure change. Using this packer system, both aperture and flow rate are directly
42 observed under various water pressures. Results indicate a slight change in fracture
43 hydraulic head leads to an observable change in aperture. This suggests that aperture
44 change should be considered when analyzing hydraulic test data from a sparsely
45 fractured rock aquifer.

46

47 **Introduction**

48 Groundwater flow through fractures is a major pathway for radioactive
49 contaminants to migrate from a subsurface waste repository to the biosphere. The cubic
50 law relates transmissivity of a fracture to the cube of its aperture; a relatively small
51 aperture change can lead to a large change in the flow rate and fracture transmissivity.
52 An aperture increase of 50%, for example, is related to a fracture transmissivity increase
53 of 338%. From the field applications of hydro-fracturing and the theoretical studies on
54 the hydromechanical behavior of a fractured rock (NRC 1996; Rutqvist and
55 Stephansson 2003), it is well-known that a large pore pressure change from injecting
56 fluid will increase the aperture and therefore the transmissivity of the fracture.
57 Increasing water pressure in a fracture leads to increased aperture and decreased contact
58 area. When the injected water pressure exceeds some threshold, the fracture suddenly
59 grows and fracture connectivity increases. Water pressures applied in hydro-fracturing
60 are typically in excess of 20 MPa (200 bar) (Walsh 1981; Dvorkin and Nur 1992; NRC
61 1996), and most laboratory- and field-scale studies on hydromechanical behavior have
62 focused on fracture changes and flow rates at water pressures of 1 ~ 10 MPa (10 ~ 100
63 bar) where the threshold is located (Alm 1999; Cornet et al. 2003; Rutqvist and
64 Stephansson 2003). Much smaller changes in water pressure are applied while
65 conducting hydrogeologic characterization.

66 It is plausible that even slight changes in water pressure may affect fracture
67 aperture and well testing results, analogous to the changes observed during hydro-
68 fracturing. There are few attempts to evaluate the hydromechanical response of a
69 fractured rock to a slight change in water pressure (Cappa et al. 2006; Svenson et al.
70 2008; Schweisinger et al. 2011). They installed the extensometers in a packed-off

71 section of boreholes in highly fractured rock aquifers, and measured the axial
72 displacements and pressures during various well tests such as slug, pulse, and pumping
73 tests. Note that the packed-off sections in their work were mostly fracture zones. By
74 assuming that an ideal fracture was in the test section and displacements occurred at that
75 fracture, they inferred aquifer characteristics from measurements through inverse
76 hydromechanical modeling. However, the observed displacements during the well tests
77 were small enough to ignore their effect on the fracture transmissivity, and the focus of
78 their work was characterization of mechanical properties using the curves for the
79 displacement as a function of water pressure.

80 In this study, we evaluate the influence of relatively small changes in water
81 pressure on fracture aperture with a series of field experiments in a sparsely fractured
82 granite aquifer. An experimental borehole is instrumented at the Korea Atomic Energy
83 Research Institute (KAERI) Underground Research Tunnel (KURT). The target fracture
84 for testing was found from the analyses of borehole logging and hydraulic tests. A
85 double packer system, which is able to directly observe the change of an aperture due to
86 water pressure change, was developed and installed in the test borehole. Using this
87 packer system, both aperture and flow rate were directly observed under various water
88 pressures.

89

90 **Motivation**

91 The KURT facility, which is in Daejeon, in the middle-western area of the
92 Korean peninsula, is a small-scale underground research facility that reaches a
93 maximum depth of 90 m below the ground surface [see Kwon et al. (2011) for site
94 description and characteristics]. Hydraulic tests were conducted in several packed-off

95 intervals of a 500 m borehole, DB-1 at the KURT (Figure 1). Table 1 shows the number
96 of fractures and estimated transmissivities from the hydraulic testing intervals. In
97 fracture zones, estimated transmissivities from constant head withdrawal tests and the
98 recovery tests are similar. In test intervals with fewer fractures, transmissivities from
99 constant head withdrawal test results are approximately an order of magnitude smaller
100 than those from the recovery, and the difference between the test results becomes larger
101 as the number of fractures in the packed-off interval decreases. Several phenomena are
102 potential causes of this. However, because imposed hydraulic gradients and
103 groundwater flow direction are equal between constant head withdrawal and recovery
104 tests, the cause cannot be the nonlinear groundwater flow in a fracture due to high
105 imposed hydraulic gradients (Ji et al. 2008) or the trapping zone effect from the
106 directional anisotropy of flow (Boutt et al. 2006).

107 Water pressure is decreasing within the formation during a constant head
108 withdrawal test while it is increasing during a recovery test. We propose that this
109 difference in water pressure causes a small aperture change that explains the differences
110 between estimated transmissivity values from the two types of hydraulic test results. To
111 verify this idea, we directly observe the change in fracture aperture when we change the
112 water pressure in an interval.

113

114 **Approach**

115 For direct observation of the fracture aperture during a test, we designed and
116 built a special double packer system composed of three parts (Figure 2): an outer pipe,
117 an inner pipe and a clear acrylic pipe. Eight rubber packers are used to mechanically
118 isolate a 90 cm long specific zone in a borehole, and are attached to the outer pipe. A 30

119 cm long x 13 cm wide observation window is located in the specific zone between the
120 upper and lower packers in the outer pipe (Figures 2a and 2d). The outer pipe has a
121 diameter of 9.8 cm. The inner pipe with a diameter of 8.2 cm is a passage for a borehole
122 camera and cables, and a barrier to shut out the influence of the assigned water pressure
123 to the test zone on the camera (Figure 2b). The inner pipe is coupled with the acrylic
124 pipe for direct observation of a fracture using a borehole camera (Figure 2c), and placed
125 inside the outer pipe. The outer and inner pipes are made of stainless steel and can be
126 extended to the target zone using blank pipe of the same diameter.

127 Borehole TB-5 at the KURT field site was selected as the test borehole for in-
128 situ experiments (Figure 1). It is 30 m deep and 10.2 cm (4 inches) in diameter, and is
129 completed in massive Jurassic granite. Acoustic televiewing was used to locate the test
130 zone and target fracture. Hydraulic tests (constant-head withdrawal and recovery) were
131 conducted in the test zone to check the suitability of the target fracture for the
132 experiments. The constant-head withdrawal test results were analyzed with the Moye
133 (Batu 1998), Jacob-Lohman (Jacob and Lohman 1952), and straight-line models
134 (Lohman 1972); the recovery test results are analyzed using the Horner model (Horne
135 1995).

136 After locating the test zone and target fracture, the water injection tests were
137 conducted. Figure 3 is a schematic of the experimental setup for observation of the
138 aperture under various water pressures. The pressurized water was injected into the test
139 zone through the space between the outer and inner pipes using a constant pressure
140 injection pump, maintaining the desired water pressure. A borehole camera (R-CAM
141 1000, Laval Underground Survey Inc.) was inserted into the inner pipe to record the
142 aperture change of the target fracture during the experiment. A flow meter and pressure

143 gauge were installed between the injection pump and the injection hole in the outer pipe
144 to measure the established water pressure and the injection rate into the target zone. The
145 tubing that links the injection pump to the injection hole is stainless steel to prevent
146 head loss, and the inner pipe is filled with water to minimize the optical distortion at the
147 acrylic pipe. The imposed water pressures were 2, 3, 4, and 5 bars; the initial water
148 pressure during the all experiments was 0.1 bars. Water injection tests were repeated
149 three times at each pressure. The selected differences between the imposed and initial
150 water pressures are common in hydraulic tests conducted in fractured rock aquifers
151 (Beauheim et al. 2004). The vertical separation distance between two near-planar
152 surfaces, according to some pre-established Cartesian coordinate system, was used as
153 the fracture aperture in the analyses (Konzuk and Kueper 2004).

154

155 **Results and Discussions**

156 Acoustic televiewing results show that the fracture frequency, defined as the
157 number of fractures per unit length of the borehole, is 2.6 m^{-1} , and that fractures are
158 evenly distributed along the borehole. Figure 4 shows the borehole logging result at the
159 section 26.0 – 30.0 m below the top of the casing (TOC). Fractures crossing TB-5
160 borehole were identified from the amplitude distribution of the measured acoustic wave.
161 Based on the borehole logging data, the packed-off section 28.2 – 29.1 m below TOC
162 was selected as the test zone because it has a single fracture, allowing intensive
163 observation and analysis of the target fracture.

164 Figure 5 indicates the results of the hydraulic tests. During constant-head
165 withdrawal tests, the hydraulic head in the test zone was instantaneously decreased from
166 an initial value to the assigned head and was kept constant. The initial outflow rate was

167 at a maximum. During the test the outflow and pressure were monitored as outflow
168 decayed to a steady value. The initial and assigned heads were 22.7 and 11.2 m,
169 respectively, in our constant-head withdrawal test. During the recovery tests the
170 groundwater outflow was stopped; hydraulic head was monitored while it recovered to
171 the original pre-test value. From the constant head withdrawal test, the transmissivity of
172 the test zone is estimated as 3.6×10^{-9} , 4.8×10^{-9} and $5.2 \times 10^{-9} \text{ m}^2/\text{s}$ with the Moye
173 (Batu 1998), Jacob-Lohman (Jacob and Lohman 1952) and straight line models
174 (Lohman 1972), respectively, which are at least a factor of 0.2 smaller than the
175 estimated transmissivity from the recovery test ($2.7 \times 10^{-8} \text{ m}^2/\text{s}$). This difference cannot
176 be due to the use of different models for interpreting the data. This result indicates that
177 the proposed test zone and target fracture are suitable for the experiments.

178 To reveal the relation between the water pressure and aperture, water injection
179 tests were conducted, and the aperture and steady-state injection rate of water were
180 measured while various water pressures were imposed. Figure 6a shows the measured
181 hydraulic heads and injection rates during the experiment when we imposed water
182 pressure of 5 bars. The hydraulic head was initially 1.4 m. When the experiment began,
183 it was abruptly increased to 50.5 m, and kept constant, although it oscillated slightly due
184 to the injection pump. The injection rate was greatest at the beginning of the experiment,
185 and stabilized at $1.06 \times 10^{-3} \text{ m}^3/\text{d}$. The response of the target fracture was recorded
186 during the test using the borehole camera, and Figures 6b-c are the snapshots of the
187 aperture before the water injection and after reaching steady state flow, at 319 minutes
188 elapsed time. Immediately after a water pressure of 5 bars was imposed, the aperture
189 was on average increased by a factor of 1.25 ± 0.01 . Then, as time elapsed from the
190 initial pressurization, the aperture gradually became larger. The aperture stabilized at

191 about 20 minutes elapsed time. The stabilized aperture was on average about a factor of
192 1.44 ± 0.03 larger than the initial aperture (Figure 6d).

193 When water pressures of 2, 3 and 4 bars were applied, changes in aperture were
194 also observed. Changes were similar to the case where the water pressure of 5 bars was
195 imposed: the apertures increased rapidly at the beginning of the experiments, and
196 stabilized after a gradual increase. Figure 7 shows the relation between the applied
197 hydraulic head and the stabilized aperture change. When water pressures of 2, 3 and 4
198 bars were applied, the hydraulic heads converged to 21.4, 29.2 and 37.5 m, respectively,
199 and the apertures finally increased on average by factors of 1.22 ± 0.02 , 1.27 ± 0.03 and
200 1.29 ± 0.06 , respectively, from the initial aperture.

201 Walsh (1981) reviewed the effect of the confining pressure on fracture
202 permeability during hydro-fracturing, and described the relation between the confining
203 pressure and aperture for a fracture having random fracture surface topography as

$$204 \frac{de}{dp} = \frac{\sqrt{2}m}{p} \quad (1)$$

205 where $2e$ is the aperture, p is the confining pressure, and m is the standard deviation of
206 the asperity heights. Hence, it is expected that the aperture increases linearly with the
207 natural log of imposed pressure on a fracture, and our data generally follows this
208 expectation (see Figure 7). From the fitted straight line to our data, the stabilized
209 aperture of the target fracture during the hydraulic tests can be estimated: if the
210 hydraulic heads at the fracture are 11.2 and 22.7 m, the apertures are a factor of 1.05
211 and 1.21 larger than that at the hydraulic head of 1.4 m, respectively. From this
212 estimation and the cubic law, it can be inferred that the estimated transmissivity of the
213 test zone from the constant head withdrawal test is approximately a factor of 0.6 smaller
214 than that from the recovery test by the aperture changes. This estimated discrepancy

215 between the transmissivities from the constant head withdrawal and recovery tests is
216 smaller than that observed during the hydraulic tests, which could be a result of ignoring
217 the change in contact area and tortuosity due to aperture change in the estimation
218 (Matsuki et al. 2008).

219

220 **Summary and Conclusions**

221 Our experimental results indicate that relatively small changes in hydraulic
222 head during a hydraulic test can lead to fracture aperture changes. A small change in
223 aperture induces considerable changes in the estimated fracture hydraulic parameters
224 because the transmissivity is proportional to the cube of the aperture. Additionally, the
225 tortuosity in a fracture is influenced by the aperture. Tortuosity decreases with
226 increasing aperture due to a decrease in asperity contacts between the fracture walls.

227 Accurate hydrogeological characterization of a radioactive waste disposal site is
228 very important because it provides the input parameters for the safety assessment of a
229 repository and controls the safety assessment results. It is difficult to apply our results
230 directly to improving the quality of a hydraulic test for accurate hydrogeological
231 characterization because there are many factors to be considered (e.g. depth to the test
232 zone, fracture density in the test zone, mechanical properties of the host rock and
233 geometrical properties of the test fractures). Nevertheless, our results show that the
234 effects of water pressure change during a hydraulic test should be considered in test
235 design and analysis. For example, using only constant head withdrawal test data can
236 lead to underestimation of hydraulic parameters, which can potentially lead to
237 overestimation of overall repository safety during ambient pressure conditions.
238 Projection of our results to sparsely-fractured rock aquifer characterization suggests the

239 pressure-rising hydraulic test is more appropriate than the pressure-decreasing hydraulic
240 test for a conservative safety assessment of a subsurface radioactive waste repository.
241 Then, only a small disturbance of hydraulic heads from the natural condition during a
242 hydraulic test is necessary to estimate the hydraulic parameters close to truly
243 representative values.

244

245

246 **Acknowledgement**

247 This work was supported by the Korean Nuclear Energy R&D program of the Ministry
248 of Science and Technology, Korea. The authors thank the editor-in-chief and three
249 anonymous reviewers for their constructive comments.

250 Sandia National Laboratories is a multi-program laboratory managed and operated by
251 Sandia Corporation, a wholly owned subsidiary of Lockheed Martin Corporation, for
252 the U.S. Department of Energy's National Nuclear Security Administration under
253 contract DE-AC04-94AL85000.

254

255 **References**

256 Alm, P. 1999. *Hydro-mechanical behavior of a pressurized single fracture: an in situ*
257 *experiment*. Ph.D. Thesis, Chalmers University, Sweden.

258 Batu, V. 1998. *Aquifer hydraulics: A comprehensive guide to hydrogeologic data*
259 *analysis*. New York: John Wiley & Sons.

260 Beauheim, R.L., R.M. Roberts, and J.D. Avis 2004. Well testing in fractured media:
261 flow dimensions and diagnostic plots. *J. Hydraulic Res.* 42: 69-76.

262 Boutt, D.F., G. Grasselli, J.T. Fredrich, B.K. Cook, and J.R. Williams 2006. Trapping
263 zones: The effect of fracture roughness on the directional anisotropy of fluid flow
264 and colloid transport in a single fracture. *Geophys. Res. Lett.* 33: L21402,
265 doi:10.1029/2006GL027275.

266 Cappa, F., Y. Guglielmi, J. Rutqvist, C.-F. Tsang, and A. Thoraval 2006.
267 Hydromechanical modeling of pulse tests that measure fluid pressure and fracture
268 normal displacement at Coaraze Laboratory site, France. *Int. J. Rock Mech. Min.*
269 *Sci.* 43: 1062-1082.

270 Cornet, F.H., L. Li, J.-P. Hulin, I. Ippolito, and P. Kurowski 2003. The
271 hydromechanical behaviour of a fracture: an in situ experimental case study. *Int. J.*
272 *Rock Mech. Min. Sci.* 40: 1257-1270.

273 Dvorkin, J., and A. Nur 1992. Filtration fronts in pressure compliant reservoirs.
274 *Geophys.* 57: 1089-1092.

275 Horne, R.N. 1995. *Modern well test analysis: A computer-aided approach*, 2nd Ed. Palo
276 Alto, CA: Petroway, Inc.

277 Jacob, C.E., and S.W. Lohman 1952. Nonsteady flow to a well of constant drawdown in
278 an extensive aquifer. *Transactions*, 33: 559-569.

279 Ji, S.-H., H.-B. Lee, I.W. Yeo, and K.-K. Lee 2008. Effect of nonlinear flow on DNAPL
280 migration in a rough-walled fracture. *Water Resour. Res.* 44: W11431,
281 doi:10.1029/2007WR006712.

282 Konzuk, J.S., and B.H. Kueper 2004. Evaluation of cubic law based models describing
283 single-phase flow through a rough-walled fracture. *Water Resour. Res.* 40:
284 W02402, doi:10.1029/2003WR002356.

285 Kwon, S., W.J. Cho, and J.W. Choi 2011. Initial thermal conditions around an
286 underground research tunnel at shallow depth. *Int. J. Rock Mech. Min. Sci.* 48: 86-
287 94.

288 Lohman, S.W. 1972. *Ground-water hydraulics, U.S. Geological Survey Professional
289 Paper 708*. Washington, DC: US Government Printing Office.

290 National Research Council (NRC) 1996. *Rock Fractures and Fluid Flow:
291 Contemporary Understanding and Applications*. Washington, DC: National
292 Academy Press.

293 Matsuki, M., E.Q. Wang, A.A. Giwelli, and K. Sakaguchi 2008. Estimation of closure
294 of a fracture under normal stress based on aperture data. *Int. J. Rock Mech. Min.
295 Sci.* 45: 194-209.

296 Rutqvist, J., and O. Stephansson 2003. The role of hydromechanical coupling in
297 fractured rock engineering. *Hydrogeol. J.* 11: 7-40.

298 Schweisinger, T., E.J. Svenson, and L.C. Murdoch 2011. Hydromechanical behavior
299 during constant rate pumping tests in fractured gneiss. *Hydrogeol. J.* 19: 963-980.

300 Svenson, E., T. Schweisinger, and L.C. Murdoch 2008. Field evaluation of the
301 hydromechanical behavior of flat-lying fractures during slug tests. *J. Hydrol.* 359:
302 30-45.

303 Walsh, J.B. 1981. Effect of pore pressure and confining pressure on fracture
304 permeability. *Int. J. Rock Mech. Min. Sci. Geomech. Abstr.* 18: 429-435.

305

306

307 **Figure caption**

308 **Figure 1.** Layout of the KURT and the location of the test borehole, TB-5.

309 **Figure 2.** Designed double packer system. (a) outer pipe with packers; (b) inner pipe for
310 a borehole camera and cables; (c) acrylic pipe for direct observation of fractures; and (d)
311 assembled double packer system.

312 **Figure 3.** Schematic of the experimental set up.

313 **Figure 4.** Borehole logging result at the section 26.0 – 30.0 m below TOC.

314 **Figure 5.** Measured hydraulic heads and flow rates during the constant head withdrawal
315 and recovery tests.

316 **Figure 6.** (a) Measured hydraulic heads and injection rates when the water pressure of 5
317 bars is imposed to the test zone. Snapshots of the target fracture (b) before imposing the
318 pressure; (c) at an elapsed time of 319 minutes from imposing; and (d) changes of
319 apertures during the experiment. The black lines indicate a sketch of the aperture in the
320 white rectangle in Figure 3b before the experiment, and the red, green, and blue ones are
321 after 30 seconds, 10 minutes, and 20 minutes after a pressure of 5 bars is imposed,
322 respectively.

323 **Figure 7.** Semi-log relation between the applied hydraulic head and the change of
324 aperture from the initial one at the hydraulic head of 1.4 m. The y-axis values indicate
325 the factor increase in fracture aperture. The dots and bars are the averages and standard
326 deviations of the aperture changes at each applied hydraulic head, respectively. The
327 dashed line in the graph is the fitted straight line to the data.

328

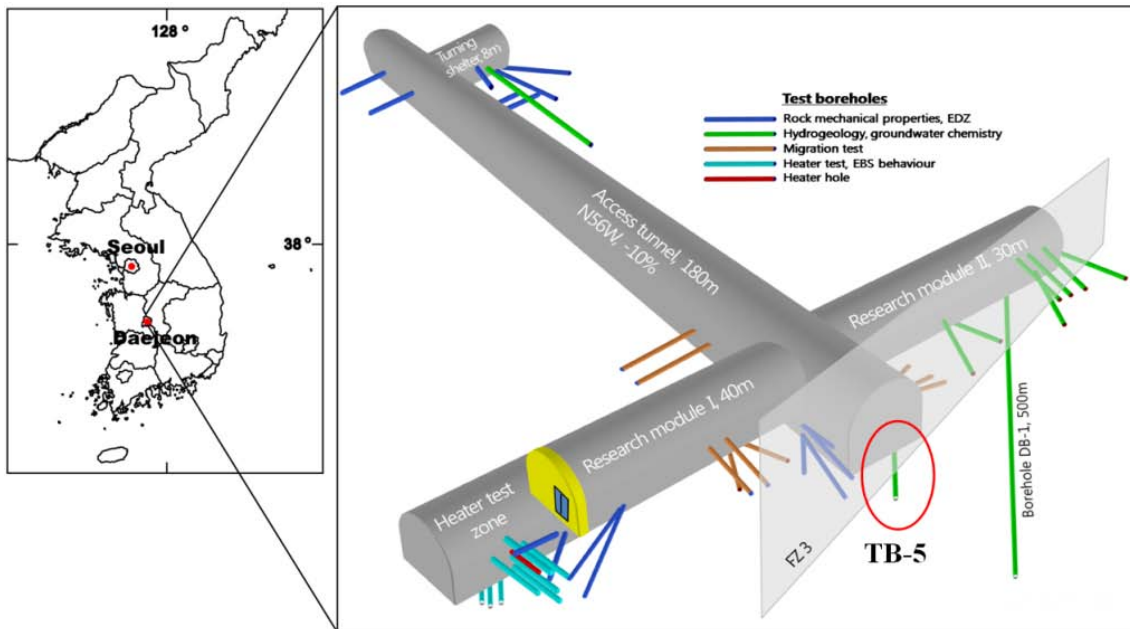
329 **Table 1.** The number of fractures and estimated interval transmissivities from the
 330 constant head withdrawal and recovery tests conducted at several packed-off intervals in
 331 borehole DB-1 installed at KURT.

Test interval (meters from TOC)	Fracture frequency [m ⁻¹]	Estimated interval transmissivity [m ² /sec]			
		Moye	Jacob- Lohman	Straight line	Recovery test Horner
8 - 23	Fracture zone	2.8x10 ⁻⁵	8.2x10 ⁻⁵	3.6x10 ⁻⁵	1.2x10 ⁻⁵
43.5 - 59.5	Fracture zone	1.5x10 ⁻⁶	1.1x10 ⁻⁶	1.1x10 ⁻⁶	9.4x10 ⁻⁷
65 - 85	2.75	1.6x10 ⁻⁷	1.3x10 ⁻⁷	7.4x10 ⁻⁸	1.5x10 ⁻⁶
92 - 116	Fracture zone	8.2x10 ⁻⁷	6.9x10 ⁻⁷	9.7x10 ⁻⁷	6.3x10 ⁻⁷
125 - 145	3.10	1.1x10 ⁻⁷	6.3x10 ⁻⁸	4.6x10 ⁻⁸	5.7x10 ⁻⁷
150 - 160.5	Fracture zone	5.1x10 ⁻⁸	3.6x10 ⁻⁸	3.8x10 ⁻⁸	1.6x10 ⁻⁷
161 - 181	6.85	1.1x10 ⁻⁷	9.1x10 ⁻⁸	8.2x10 ⁻⁸	4.0x10 ⁻⁷
183 - 194	Fracture zone	1.1x10 ⁻⁷	1.3x10 ⁻⁷	1.8x10 ⁻⁷	1.7x10 ⁻⁷
201.5 - 226	Fracture zone	6.7x10 ⁻⁶	1.5x10 ⁻⁵	2.1x10 ⁻⁵	1.0x10 ⁻⁴
237 - 247	Fracture zone	2.1x10 ⁻⁶	5.4x10 ⁻⁶	8.5x10 ⁻⁶	4.5x10 ⁻⁵
251 - 271	0.80	1.7x10 ⁻⁷	5.8x10 ⁻⁸	6.3x10 ⁻⁸	1.0x10 ⁻⁶
279 - 293	Fracture zone	3.9x10 ⁻⁸	3.8x10 ⁻⁸	5.0x10 ⁻⁸	8.8x10 ⁻⁷
291 - 311	2.45	5.9x10 ⁻⁸	3.0x10 ⁻⁸	2.9x10 ⁻⁸	5.6x10 ⁻⁸
311 - 331	0.80	3.1x10 ⁻⁸	1.3x10 ⁻⁸	1.5x10 ⁻⁸	6.1x10 ⁻⁸
331 - 351	0.40	5.7x10 ⁻⁸	3.1x10 ⁻⁸	3.5x10 ⁻⁸	1.5x10 ⁻⁷
351 - 371	0.75	5.6x10 ⁻⁸	3.3x10 ⁻⁸	3.2x10 ⁻⁸	3.5x10 ⁻⁷
371 - 391	0.55	6.0x10 ⁻⁸	4.1x10 ⁻⁸	3.4x10 ⁻⁸	4.4x10 ⁻⁷
391 - 411	0.20	5.9x10 ⁻⁸	3.0x10 ⁻⁸	3.3x10 ⁻⁸	1.8x10 ⁻⁷
411 - 431	0.40	4.9x10 ⁻⁸	3.0x10 ⁻⁸	3.4x10 ⁻⁸	3.4x10 ⁻⁷
431 - 451	0.20	4.1x10 ⁻⁸	5.1x10 ⁻⁸	2.5x10 ⁻⁸	4.5x10 ⁻⁷
451 - 471	0.80	5.5x10 ⁻⁸	5.4x10 ⁻⁸	3.4x10 ⁻⁸	2.8x10 ⁻⁷
471 - 491	0.10	5.3x10 ⁻⁸	7.6x10 ⁻⁸	3.3x10 ⁻⁸	3.7x10 ⁻⁷

332

333

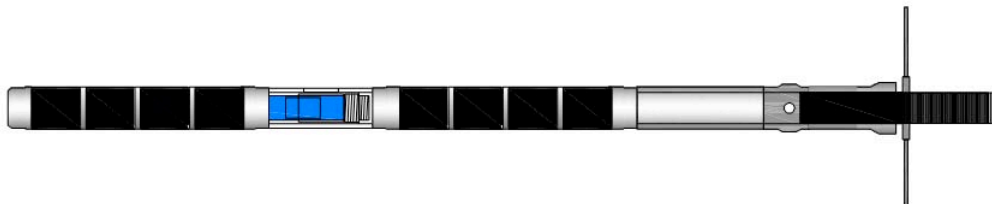
334 Fig. 1.



335

336 Fig. 2

337 (a)



338

339 (b)



340

341 (c)



342

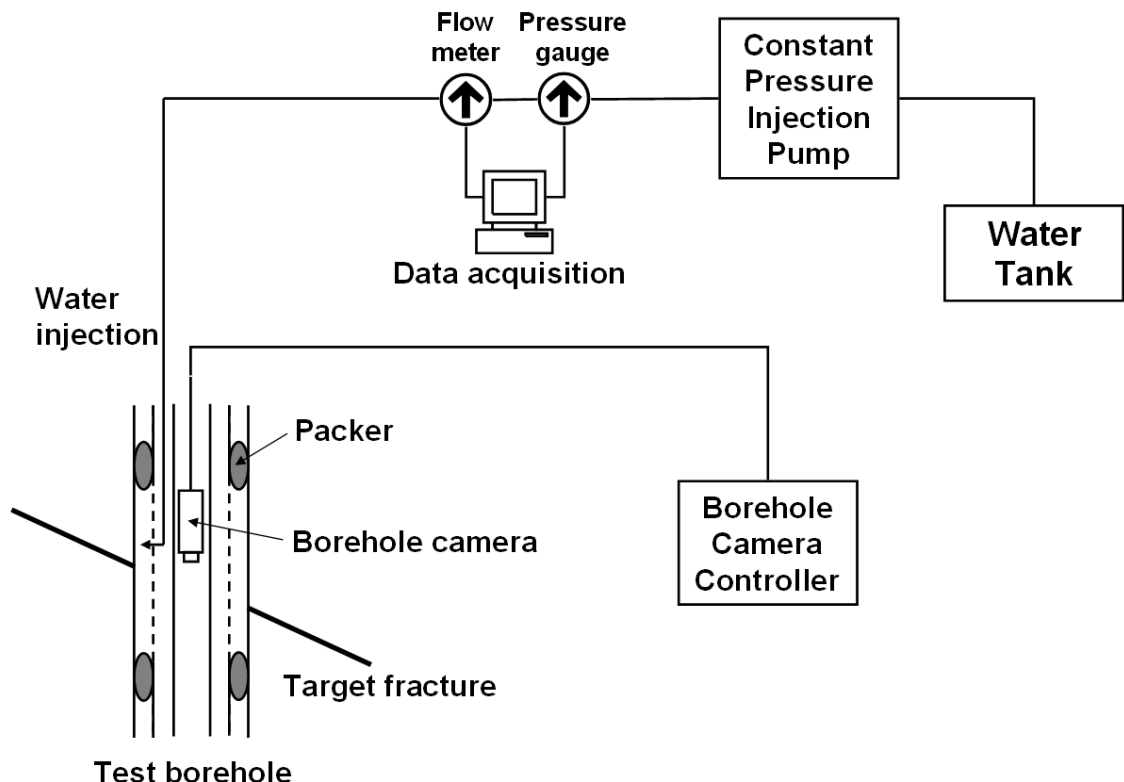
343 (d)



344

345

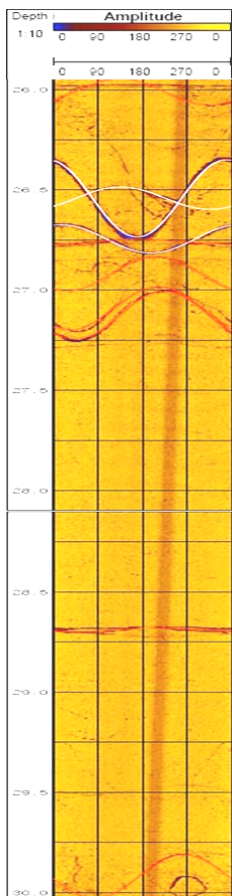
346 Fig. 3



347

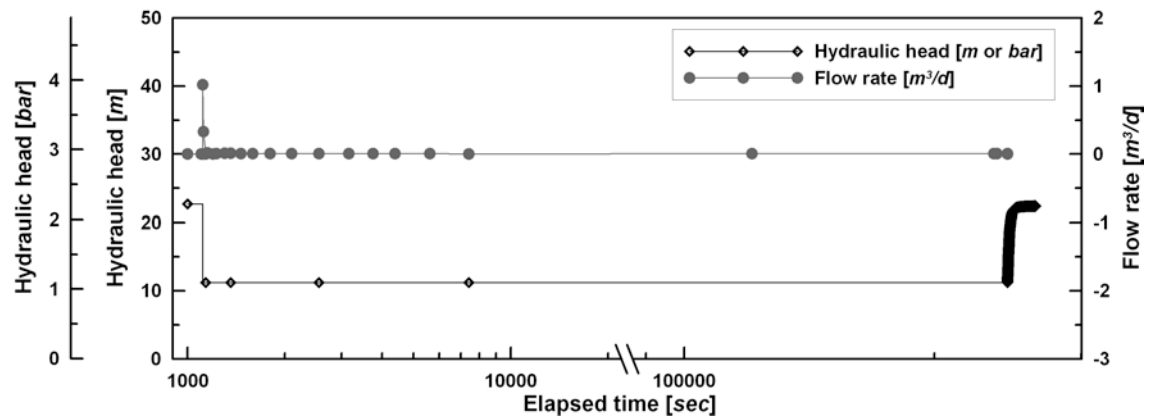
348

349 Fig. 4.



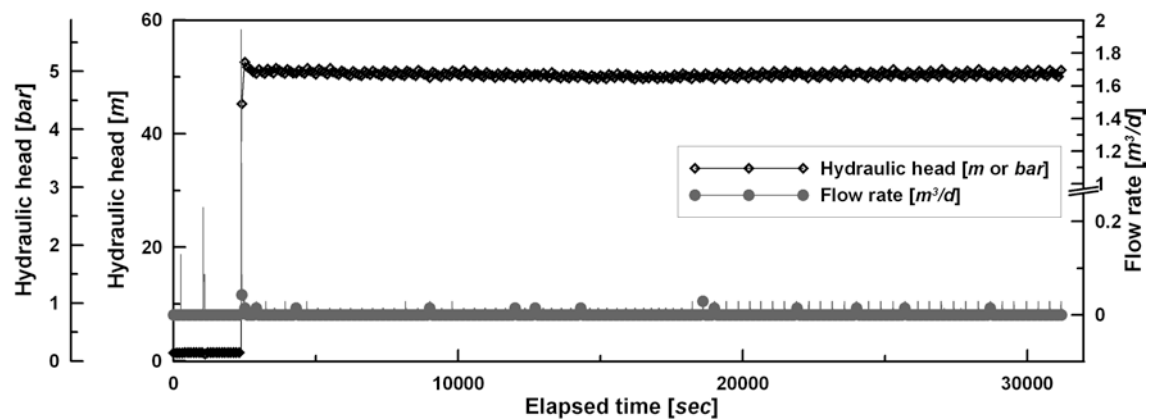
350
351

352 Fig. 5.

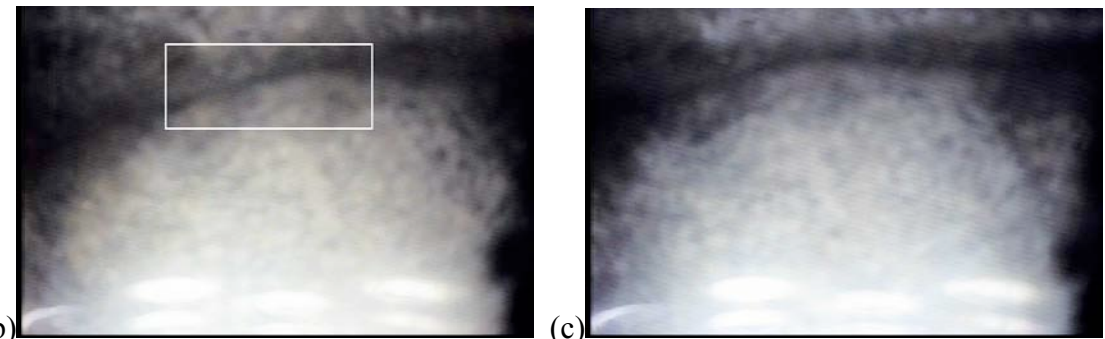


356 Fig. 6

357 (a)



358



359

(b)

(c)

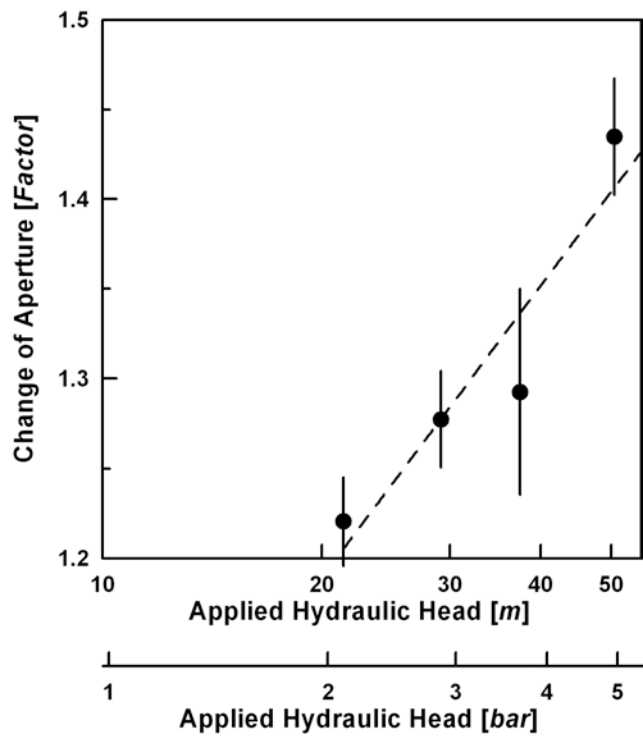
360 (d)

Aperture at ET of 20 min
Aperture at ET of 10 min
Aperture at ET of 30 sec
Initial aperture

361

362

363 Fig. 7



364

365